

Evolution of Caledonian deformation fabrics under eclogite and amphibolite facies at Vårdalsneset, Western Gneiss Region, Norway

A. K. ENGVIK¹ AND T. B. ANDERSEN²

¹Mineralogical-Geological Museum, Sarsgt. 1, 0562 Oslo, Norway (ane.engvik@toyen.uio.no), and ²Department of Geology, PO Box 1047 Blindern, 0316 Oslo, Norway

ABSTRACT The Vårdalsneset eclogite situated in the Western Gneiss Region, SW Norway, is a well preserved tectonite giving information about the deformation regimes active in the lower crust during crustal thickening and subsequent exhumation. The eclogite constitutes layers and lenses variably retrograded to amphibolite and is composed of garnet and omphacite with varying amounts of barroisite, actinolite, clinozoisite, kyanite, quartz, paragonite, phengite and rutile. The rocks record a five-stage evolution connected to Caledonian burial and subsequent exhumation. (1) A prograde evolution through amphibolite facies ($T = 490 \pm 63$ °C) is inferred from garnet cores with amphibole inclusions and bell-shaped Mn profile. (2) Formation of L>S-tectonite eclogite ($T = 680 \pm 20$ °C, $P = 16 \pm 2$ kbar) related to the subduction of continental crust during the Caledonian orogeny. Lack of asymmetrical fabrics and orientation of eclogite facies extensional veins indicate that the deformation regime during formation of the L>S fabric was coaxial. (3) Formation of sub-horizontal eclogite facies foliation in which the finite stretching direction had changed by approximately 90°. Disruption of eclogite lenses and layers between symmetric shear zones characterizes the dominantly coaxial deformation regime of stage 3. Locally occurring mylonitic eclogites ($T = 690 \pm 20$ °C, $P = 15 \pm 1.5$ kbar) with top-W kinematics may indicate, however, that non-coaxial deformation was also active at eclogite facies conditions. (4) Development of a widespread regional amphibolite facies foliation ($T = 564 \pm 44$ °C, $P < 10.3$ –8.1 kbar), quartz veins and development of conjugate shear zones indicate that coaxial vertical shortening and sub-horizontal stretching were active during exhumation from eclogite to amphibolite facies conditions. (5) Amphibolite facies mylonites mainly formed under non-coaxial top-W movement are related to large-scale movement on the extensional detachments active during the late-orogenic extension of the Caledonides. The structural and metamorphic evolution of the Vårdalsneset eclogite and related areas support the exhumation model, including an extensional detachment in the upper crust and overall coaxial deformation in the lower crust.

Key words: amphibolite; Caledonides; eclogite; exhumation, Western Gneiss Region.

INTRODUCTION

Fabrics can be used to unravel complex deformation histories, and, together with metamorphic information and P – T paths, can be used to reconstruct aspects of an orogenic cycle. Occurrences of high-pressure (HP) and ultra-high-pressure (UHP) assemblages in several orogenic belts demonstrate extreme crustal thickening and subduction of continental crust to mantle depths during collision (Chopin, 1984). The eclogites found at the surface today behaved metastably during uplift, and a fundamental question is how HP and UHP rocks have returned to the surface. Tectonic denudation on extensional detachments and faults is proposed as an important process for exhumation (Dewey, 1988; Platt, 1993). Exhumation has been suggested to occur by non-coaxial, extensional detachments cutting through the entire crust (Wernicke, 1985), or by extensional detachment in the upper part of the crust and overall coaxial deformation in the lower crust (Andersen & Jamtveit, 1990; Jolivet *et al.*, 1994). Thrusting, accompanied by erosion, is another possible

mechanism of exhumation (Avigad, 1992). A model that excludes orogenic extension is proposed for the southern Urals (Chemenda *et al.*, 1997), and is based on buoyancy forces enhancing exhumation of HP rocks by both reverse and normal faulting. While upper and middle crustal extensional faults and detachments are commonly preserved, textures and structures of lower crustal rocks can only be studied in deeply denuded orogenic belts such as the Norwegian Caledonides which enlighten the processes of subduction and subsequent exhumation of high-pressure rocks.

The structure of the Norwegian Caledonides is dominantly the product of the Silurian continental collision between Baltica and Laurentia (Torsvik *et al.*, 1996) and the late- to post-orogenic extension of the orogen in the Late Silurian to Devonian (Andersen, 1998). The rocks of the Western Gneiss Region (WGR) experienced eclogite facies conditions during the Caledonian orogeny (Griffin *et al.*, 1985). At present, the WGR constitutes a high-pressure metamorphic core complex separated from the overlying Caledonian

nappes by late- and post-Caledonian extensional shear zones and normal faults in the upper and middle crust (Norton, 1987; Andersen & Jamtveit, 1990; Milnes *et al.*, 1997). Other studies propose thrust imbrication to be important in the WGR (Cuthbert *et al.*, 1983; Wain, 1997), while a transtensional model for exhumation was proposed by Krabbendam & Dewey (1998). The rocks in the WGR are of Middle Proterozoic age (about 1750–900 Ma) (Kullerud *et al.*, 1986; Tucker *et al.*, 1987). The eclogite facies metamorphism is dated by U–Pb and Sm–Nd methods at 420–400 Ma, although some older ages (440 Ma) have been reported (Griffin & Brueckner, 1980, 1985; Gebauer *et al.*, 1985; Tucker in Lutro *et al.*, 1997). The eclogites are variably overprinted by amphibolite and greenschist facies assemblages (Krogh, 1980; Cotkin *et al.*, 1988). The amphibolite facies metamorphism is associated with both deformation and static retrogression during decompression of the high-pressure rocks (Andersen & Jamtveit, 1990).

The mineralogy and petrology of the eclogites in WGR have been studied extensively (see reviews by Krogh & Carswell, 1995; Smith, 1995; and references therein). *P–T* estimates of coesite-bearing eclogites from the WGR indicate that pressures of 28 kbar were attained in the north-western sections of WGR (Wain, 1997). The identification of diamond-bearing eclogite and gneisses in the north-western parts of WGR indicates pressures of more than 30 kbar during the Caledonian orogeny, implying subduction of continental crust lithologies to more than 90 km depth (Dobrzhinetskaya *et al.*, 1995). The T_{\max} of the eclogite facies metamorphism increases in the north-westerly direction from about 600 °C in the Sunnfjord area to more than 750 °C in the NW coastal areas (Griffin *et al.*, 1985).

The Vårdalsneset eclogite (Fig. 1) is structurally positioned in the upper part of the WGR in Sunnfjord, approximately 3 km below the extensional brittle fault capping the Nordfjord-Sogn Detachment (NSD). The eclogite is positioned in 'zone 3', dominated by coaxial deformation as defined by Andersen & Jamtveit (1990). The area mapped in detail comprises mainly eclogite and amphibolite within subordinate granodioritic gneisses (Fig. 2) and displays relationships between various structural and metamorphic events particularly well. The relationships between structures of the Vårdalsneset eclogite to the extensional detachment and WGR have been established by Andersen & Jamtveit (1990) and Swensson & Andersen (1991). Later folding also affecting the Devonian basins in western Norway has complicated the structure of the area (Skjerlie, 1969; Torsvik *et al.*, 1986; Krabbendam & Dewey, 1998). However, the close spatial relationship and involvement in deformation of the NSD gives a good structural control of the eclogite position related to the enveloping regional geology. Hence, the rocks at Vårdalsneset and similar eclogite facies tectonites elsewhere in the WGR have played a key role in the

evolution of theories of the late-orogenic uplift of deep crust (Dewey *et al.*, 1993; Andersen *et al.*, 1994). Andersen *et al.* (1994) developed a three-stage model for the orogenic evolution of the Caledonides deep crust, comprising eclogite facies compression followed by amphibolite facies flattening and non-coaxial extension. In the present study, we tested the models presented by Andersen *et al.* (1994) by additional detailed petrographic, metamorphic and structural analyses. Parts of the eclogite and its surroundings (400 m × 100 m) have been mapped in detail on a 5 m² grid covering the well exposed wave-washed outcrops. Chemical zonation of garnet in eclogite and amphibolite is used to integrate the metamorphic and structural evolution. The detailed observations are used to discuss the tectono-metamorphic evolution during the burial and subsequent exhumation.

PETROGRAPHY AND STRUCTURAL RELATIONS OF THE VÅRDALSNESET ECGOLITE

Eclogite facies

L > S-tectonite

The *L > S-tectonite* comprises variably disrupted eclogite lenses. The largest and best preserved body covers an area of 200 m × 100 m in the core of the eclogite. Smaller lenses (0.3–10 m) are commonly present within the foliated eclogites (Figs 2 & 3a). The largest eclogite lens is coarse-grained having a penetrative lineation and a weak foliation, with almandine-rich garnet and omphacite crystals up to several cm long. Barroisite, actinolite, phengite, paragonite, clinozoisite, quartz, kyanite and rutile also belong to the eclogite assemblage, while talc, apatite, tourmaline, carbonate and pyrite are accessory minerals (Table 1). Numerous inclusions of amphibole, quartz, plagioclase, epidote, white mica, omphacite, kyanite and rutile are found in the garnet porphyroblast.

The lineation is defined by the eclogite facies minerals that show a preferred orientation of both grain-shape anisotropy (SPO) and crystal lattice (CPO), and is dominated by omphacite together with kyanite, clinozoisite and amphibole. The euhedral garnet commonly shows oblong form parallel to the lineation (Fig. 4a). Quartz, where present, commonly occurs in pressure shadows around garnet also parallel to lineation. The lineation lies in the weak, sub-vertical foliation defined by cm-thick horizons of modal garnet variations. The penetrative mineral lineation in the large eclogite lens is dominantly sub-horizontal, trending 034° in the present reference frame (Fig. 5a). The lineation in 0.3–10 m large eclogite lenses shows some variation in orientation, but in the central parts of the lenses it averages 019°/09°, which is close to the lineation of the large eclogite lens. In comparison, mineral lineations from different eclogite lenses in the larger Dalsfjord area of Fig. 1 scatter in the same

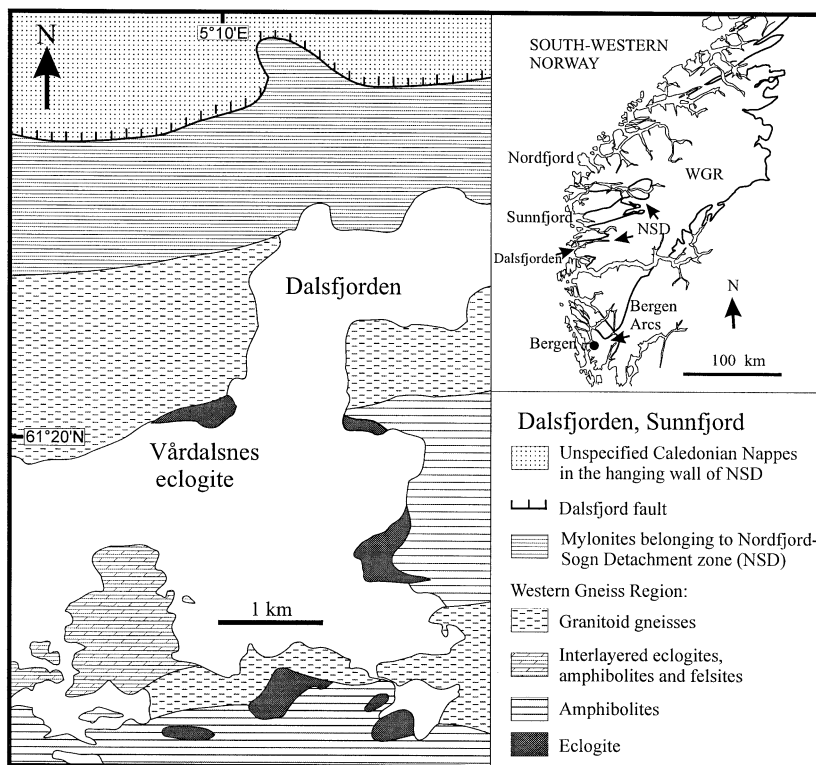


Fig. 1. Geological map of the Dalsfjord area, Sunnfjord (modified after Kildal, 1970; Andersen *et al.*, 1994; additional mapping by E. Eide, A.K. Engvik, M. Erambert and Ø. Skår).

orientation (mean $223^{\circ}03'$, Fig. 5h). The field observations and preservation of the orientation demonstrate that rotation of the smaller lenses during subsequent deformation was minimal.

Parts of the coarse-grained L>S eclogite at Vårdalsneset show a transition to a foliated eclogite. In these zones, the L>S eclogite is variably recrystallized to fine grain sizes (Fig. 4b), whereas some coarse-grained horizons and scattered porphyroclasts of omphacite and kyanite with a distinct lineation are present as remnants of the older L>S fabric. The grain size is reduced from 2–3 mm to <0.5 mm during the recrystallization. Eclogite facies micro shear bands truncate the original L>S-tectonite, with both top-E and top-W movement. The deformation and recrystallization of the coarse-grained L>S eclogite into a foliated eclogite with both top-W and top-E micro shear bands indicates E–W stretching during formation of the bulk S-fabric, i.e. stretching at a high angle to the older lineation.

Foliated eclogite and felsite

The foliated garnet+omphacite-dominated eclogite enveloping the L>S-eclogite is interlayered with felsite and characterized by a foliation wrapping the coarser lenses. The foliation generally strikes E–W with shallow northwards dips (Figs 2a & 5b), i.e. at high angle to the fabric of the L>S-tectonite. The dip-variation (Fig. 5b) is probably related to the Devonian folding

affecting the entire crustal section in West Norway (Skjerlie, 1969; Torsvik *et al.*, 1986; Krabbendam & Dewey, 1998). The foliated eclogite is generally equigranular and fine-grained, with some larger omphacite crystals, and is dominated by garnet and omphacite (Table 1). Quartz, phengite, amphibole, epidote and rutile occur in lesser amounts. Modal variations of garnet, omphacite and phengite define a compositional banding, with omphacite, epidote and phengite oriented parallel to the banding. Felsic horizons are interlayered and wrap small lenses of fine-grained eclogite. The felsites are dominated by quartz and phengite with variable amounts of epidote, garnet, symplectites of amphibole and plagioclase after omphacite and accessory rutile.

Parts of the foliated eclogite form massive layers, but in general the eclogites comprise disrupted lenses and layers between moderately dipping shear zones which form an outcrop- and map-scale anastomosing foliation (Figs 2c & 3a,b). Some eclogite layers show isoclinal folding with axial surface subparallel to the foliation. The disruption of lenses and layers by the outcrop scale shear zones (Figs 3a & 5e) shows both top-W and top-E movement. The shear zones define conjugate sets that indicate coaxial E–W stretching during formation of the eclogite facies foliation. Based on the symmetrical boudinage of the eclogite, the conjugate shear zones and the unchanged orientation of the older lineation within the boudins, the eclogite facies foliation was apparently related to dominantly

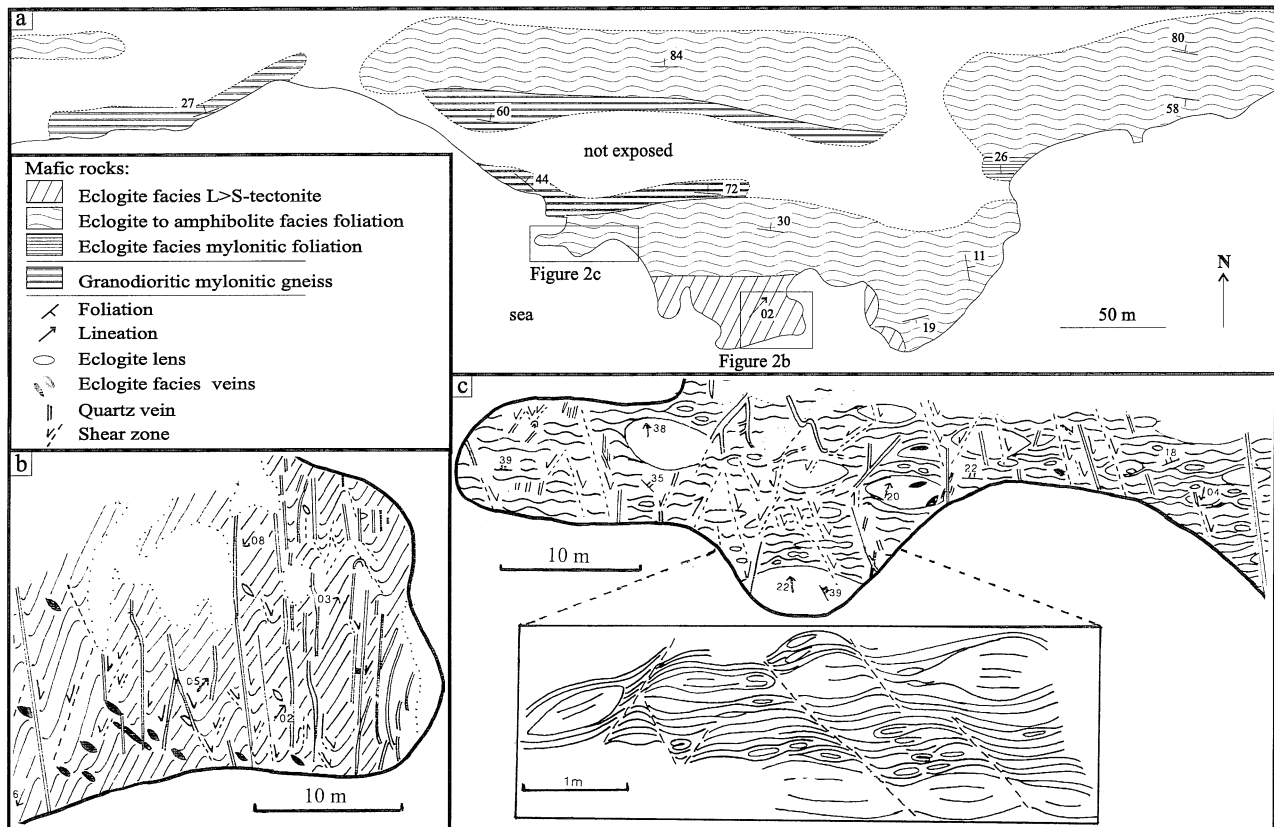


Fig. 2. (a) Lithological and fabric map of the Vårdalsneset outcrop. (b) Detailed structural map of a part of the area with eclogite L > S-tectonite. Notice the eclogite facies extensional veins oriented normal to the stretching lineation and the N–S-oriented quartz veins associated with amphibolitization. (c) Detailed structural map of a part of the eclogite to amphibolite facies foliated area showing the symmetric nature of the eclogite lenses. Notice also the N–S orientation of the L > S stretching lineation in the boudins.

subvertical shortening and E–W extension of the L > S eclogite.

In parts of the Vårdalsneset eclogite, however, a mylonite zone with both eclogite and amphibolite facies assemblages is preserved (Fig. 2a). The mylonite cuts the already foliated eclogite. In this setting, shear bands with dominant top-W sense of shear can be observed (Fig. 3c). The mylonitic eclogite is generally fine-grained (0.1–0.5 mm) and consists of syntectonic omphacite, garnet, clinozoisite and barroisite (Fig. 4c), although 4 mm porphyroblasts of barroisite and garnet occur. The strong planar foliation of the mylonitic eclogite is defined by omphacite, amphibole and clinozoisite, but thin laminae of quartz occur at the scale of the outcrop. A near E–W-trending ($080^{\circ}/16^{\circ}$) lineation of omphacite and amphibole is present on the foliation plane. The shear bands (Figs 3c & 4c) indicate that the mylonitic eclogite represents a zone that accommodates dominantly top-W movement at eclogite facies conditions. This observation suggests that zones with consistent sense of shear may locally have been present during formation of the flattening eclogite fabrics.

Eclogite facies veins

Veins dominated by kyanite and amphibole, respectively, are common in the coarse-grained eclogite (see also Andersen *et al.*, 1994). Kyanite-dominated veins consist of the host-rock minerals quartz, omphacite, white mica and garnet with accessory tourmaline and rutile, whereas the amphibole veins consist of barroisite. Mostly, the eclogite facies veins strike NW–SE, approximately normal to the lineation of the eclogite but with considerable variation in dip (Fig. 5c).

Kyanite veins are more deformed than the amphibole veins, and the internal lineation also shows a more variable orientation. However, continuity is maintained between the mineral fibre lineation in the veins and the lineation in the host rock, indicating that they formed as extensional veins (Fig. 3d). Folding of the vein margins indicates contemporaneous opening and deformation of the veins. The mineralogy, orientation and internal fabric of the kyanite veins clearly show that the veins formed at eclogite facies conditions and that they were formed and deformed simultaneously with the eclogite L > S-tectonite. The common occur-

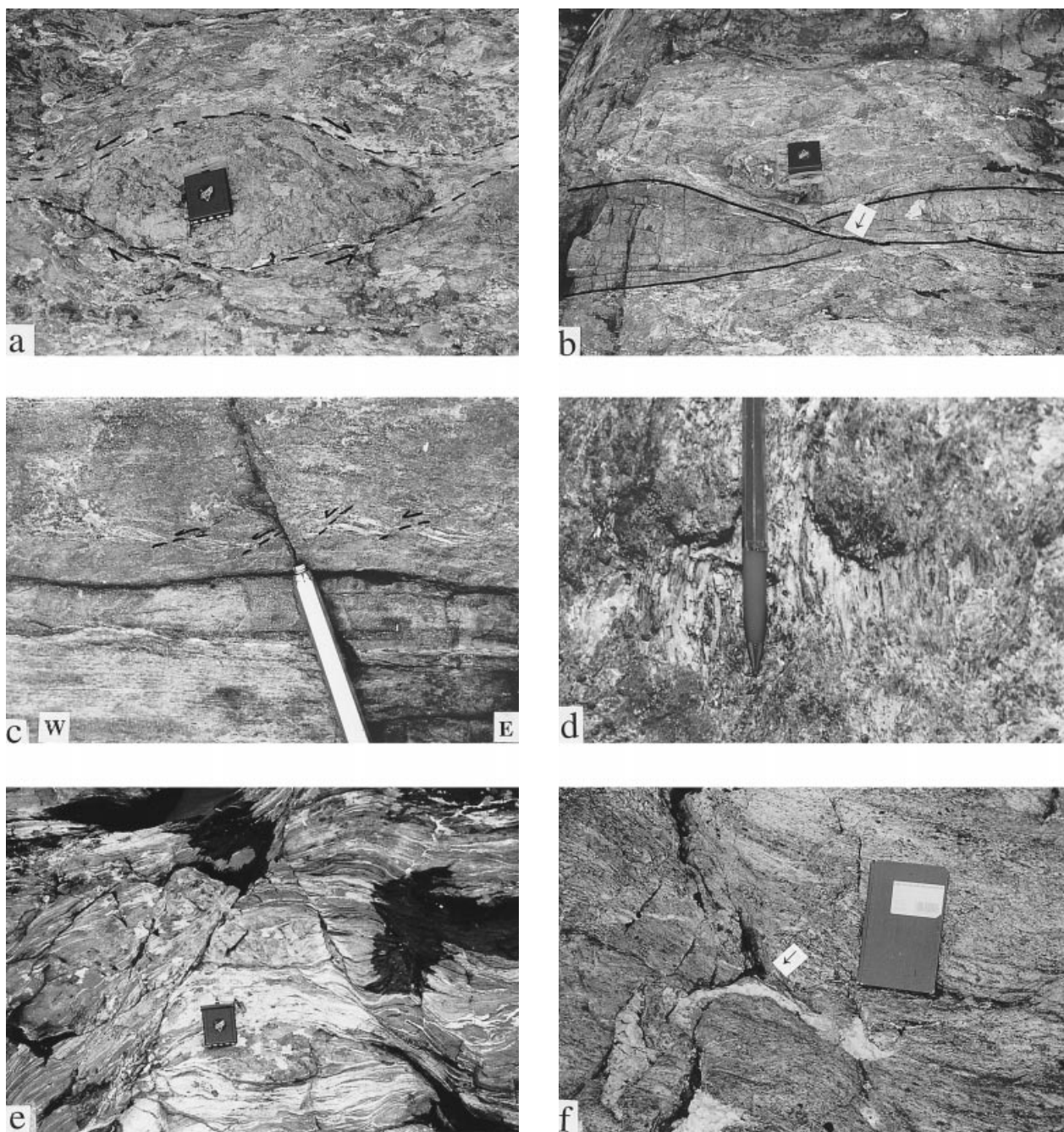


Fig. 3. (a) Small lens of lineated eclogite enveloped by anastomosing foliated (dashed line) eclogite and felsite. The stretching lineation in the lens is visible parallel to the margin of the compass. The eclogite lens is parted from the surroundings by gently dipping shear zones. (b) Moderately dipping shear zone (arrow) breaking up an eclogite layer (outlined) in anastomosing foliated eclogite and felsite. (c) Small shear bands (dashed lines) in eclogite mylonite indicating top-W deformation. (d) Kyanite-dominated hydrothermal vein. This vein also contains 3–4 cm long omphacite crystals. The mineral lineation can be traced from the eclogite through the vein (the pen indicates the trend of the mineral lineation in the eclogite and vein). (e) Conjugate set of shear zones with dextral and sinistral movement cutting the eclogite to amphibolite facies foliation at a high angle. (f) Amphibolite facies shear zone (arrow) deforming quartz vein.

rence of kyanite veins, together with hydrous phases in the eclogite, are evidence for high-pressure fluid during eclogite crystallization (Holland, 1979).

The amphibole veins have better defined margins than the kyanite veins; their opening and sealing,

however, did not cause retrogression of the eclogite wall rock. Based on the presence of barroisite as in the eclogite, their discrete margins, and their weaker deformation compared to the kyanite veins, formation of the amphibole veins was probably related to a later

Rock type	L>S-tectonite		Foliated eclogite		Amphibolite		Granodioritic gneiss	
	V5	V9	V17	V44	V22	V34	V48	V50
Omp	38.9	44.5	29.1	42.6	—	—	—	—
Grt	30.3	21.7	46.0	41.8	1.1	15.2	—	—
Amph	10.2	5.1	1.7	0.4	—	—	—	—
Amph + Pl	—	—	—	—	70.8	73.8	—	—
Pl	—	—	—	—	—	—	43.8	29.6
Kfs	—	—	—	—	—	—	17.6	9.8
Qtz	4.6	0.6	0.4	7.4	3.7	0.4	27.4	29.8
Wm	8.2	7.0	7.9	—	—	—	4.4	17.2
Ky	1.6	8.7	—	—	—	—	—	—
Ep	1.6	5.1	3.7	2.4	10.1	4.5	2.8	7.2
Bt	—	—	—	—	11.6	2.3	1.0	5.2
Chl	—	—	—	—	2.6	—	1.0	—
Rt	1.8	0.4	2.1	2.2	x	x	—	—
Tur	x	—	—	—	—	—	—	—
Ap	x	x	—	—	—	—	x	x
Cal	x	—	—	—	—	—	—	—
Opq	x	x	—	x	x	x	1.0	x
Tlc	x	—	—	—	—	—	—	—
Ttn	—	—	—	—	—	—	1.0	x

Table 1. Modal content (%) of eclogites, amphibolites and granodioritic gneiss.

Abbreviations after Kretz (1983), in addition Amph, amphibole; Wm, white mica; Opq, opaques. x, present in sample.

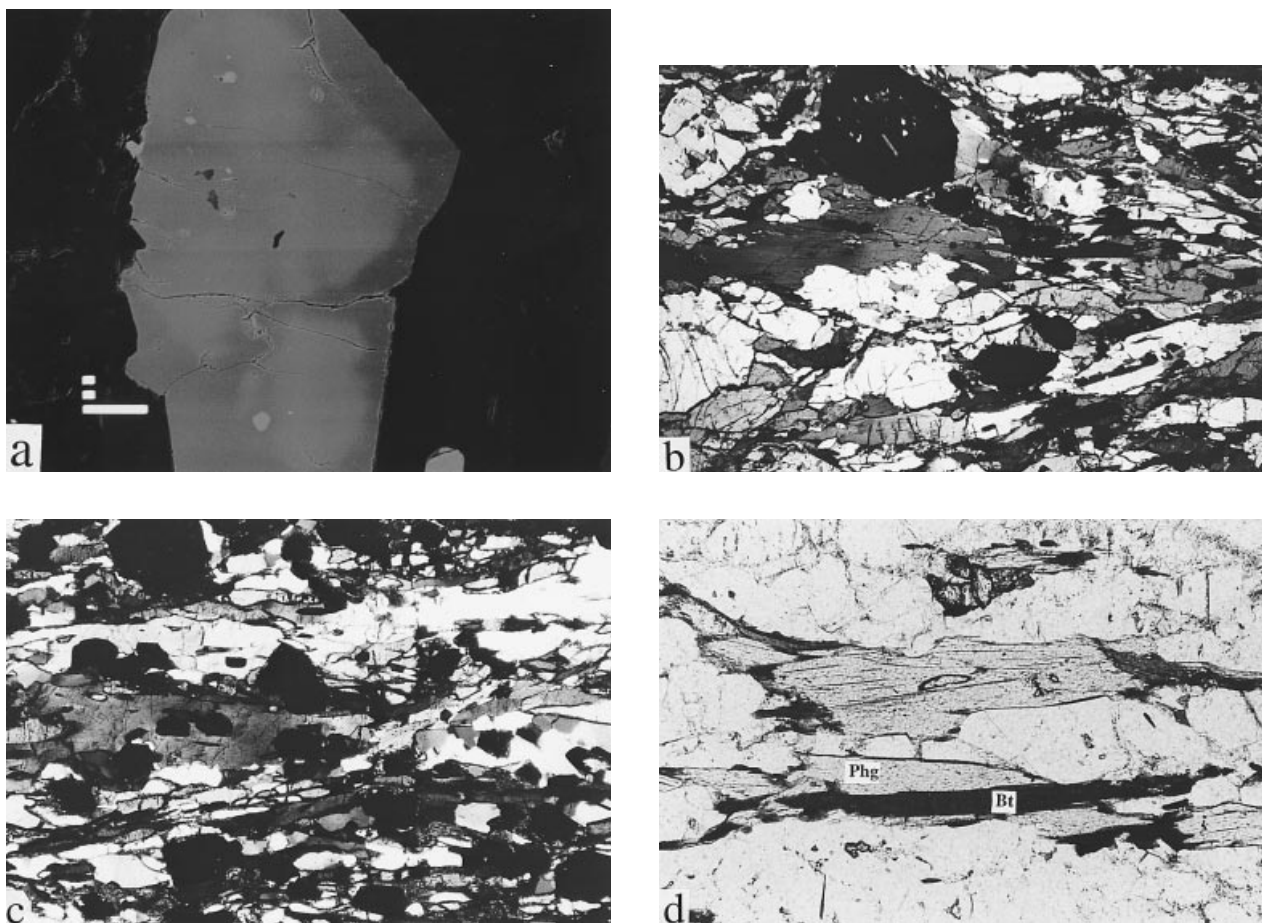


Fig. 4. (a) Oblong garnet is oriented parallel to lineation of the L>S-tectonite eclogite. Zoning fracture (dark) oriented perpendicular to the lineation direction. BSE photomicrograph, scale bar is 100 μ m. (b) Recrystallization of the coarse-grained, L>S-tectonite to fine-grained eclogite. The coarser grains of omphacite and garnet are preserved in the left part of the picture, and the finer grained in the upper right part. Photomicrograph, crossed nicols, image is 5.2 mm wide. (c) Shear band of the mylonitic eclogite indicating top-W deformation. The matrix of the mylonitic eclogite is equigranular and fine-grained but with large porphyroblasts of amphibole and garnet. Strong planar foliation is defined by omphacite, amphibole and clinozoisite. Photomicrograph, crossed nicols, image is 5.2 mm wide. (d) Phengite (Phg) and biotite (Bt) of the granodioritic gneiss. The phengite and biotite are subparallel. The growth of biotite on phengite indicates biotite formation from phengite. Photomicrograph, image is 1.3 mm wide.

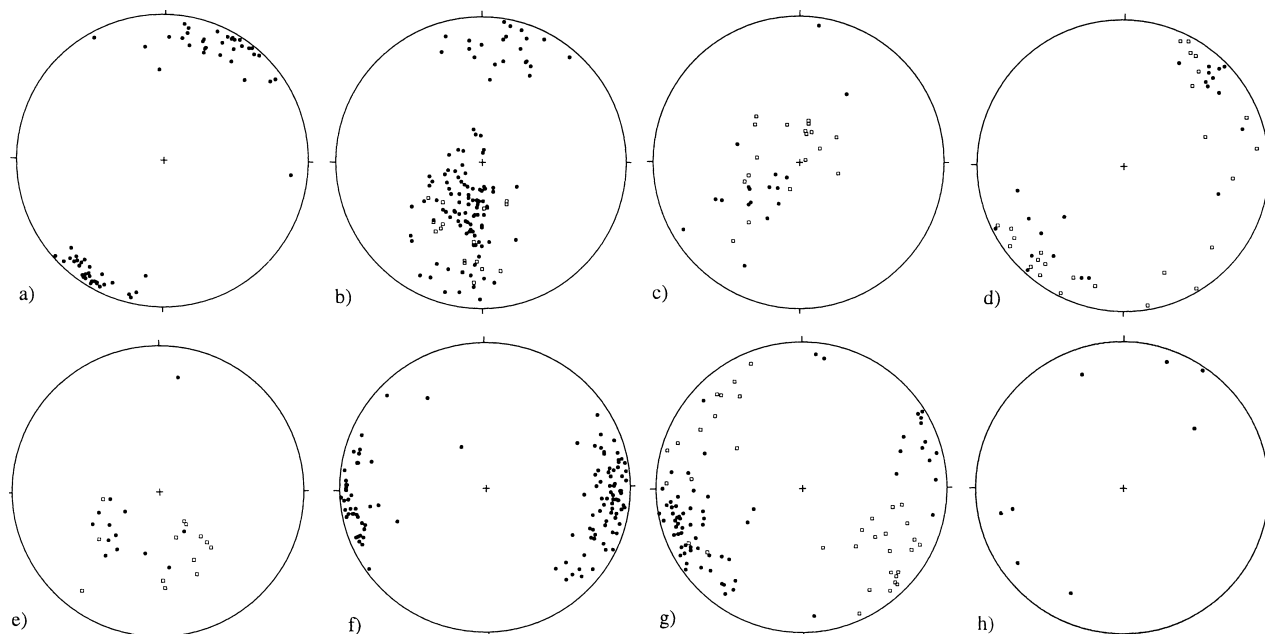


Fig. 5. Stereograms. (a) Orientation of eclogite facies lineation of the large and smaller L>S eclogite lenses ($n=64$). (b) Poles to foliation of the fine-grained eclogite (filled circles, $n=122$) and the mylonite zone (open squares, $n=20$). (c) Poles to kyanite veins (open squares, $n=19$) and amphibole veins (filled circles, $n=18$) in the large eclogite lens. (d) Orientation of lineation in kyanite veins (open squares, $n=27$) and amphibole veins (filled circles, $n=22$) in the large eclogite lens. (e) Orientation of moderately dipping shear zones of the foliated eclogite area limiting eclogite lenses and disrupting eclogite layers. Filled circles, dextral shear zones, $n=13$. Open squares, sinistral shear zones, $n=13$. (f) Poles to quartz veins, $n=115$. (g) Orientation of steep shear zones cutting the eclogite facies lineation, eclogite to amphibolite facies foliation and deforming quartz veins. Filled circles, dextral shear zones, $n=68$. Open squares, sinistral shear zones, $n=37$. (h) Orientation of eclogite facies lineation in several eclogites in the Dalsfjord area ($n=8$).

stage of fluid activity with a possibly different fluid composition. Formation of the amphibole veins, however, occurred under eclogite facies conditions and shows the same mineral stretching lineation as the L>S-tectonite and the kyanite veins.

Amphibolite facies

Amphibolites

Significant parts of the Vårdalsneset eclogite are amphibolitized, most distinctly along quartz veins cutting both the L>S and the foliated eclogites. The amphibolites after the foliated garnet + omphacite-rich eclogite are dominated by very fine-grained symplectites of magnesiohornblende to tschermakitic amphibole and plagioclase after the omphacite or by more recrystallized magnesiohornblende prisms. The eclogite facies garnet reacts to amphibole and chlorite, whereas rutile is replaced by ilmenite. White mica of the eclogite facies felsic horizons reacts partly or completely to biotite and feldspar.

The amphibolitization of the kyanite-rich eclogite occurs along both grain boundaries and fractures with similar orientation to the quartz veins. Omphacite is replaced by symplectites of diopside or amphibole and

plagioclase, or in pervasively retrogressed parts by larger amphibole crystals. Garnet is partly or completely pseudomorphed by chlorite, plagioclase and some amphibole, biotite and epidote. Kyanite breaks down to margarite, the Ca being supplied from nearby clinozoisite. Clinozoisite shows alteration to Fe-enriched epidote and calcite. White mica breaks down to plagioclase, margarite or recrystallized white mica.

The foliation of the amphibolites is subparallel to the eclogite facies foliation described above. Oriented biotite, epidote and recrystallized amphibole define a foliation of variable intensity both in the amphibolites and interlayered felsites. Biotite and epidote are commonly concentrated in bands. More intensely deformed amphibolites in shear zones underwent more comprehensive recrystallization and neomineralization. Euhedral amphibole prisms with a strong preferred orientation occur together with parallel rods of plagioclase.

Mylonitic granodioritic gneiss

The granodiorite (Fig. 2a) is a strongly foliated, fine-grained, mylonitic gneiss containing phengite and variable amounts of biotite, epidote, green amphibole and apatite, titanite, garnet and opaques as accessories

(Table 1). Biotite occurs along the rims of phengite indicating neo-mineralization after phengite (Fig. 4d). Epidote and micas, both biotite and phengite, define the foliation, together with bands of quartz and occasionally titanite. Modal variation of the mafic minerals gives the mylonitic gneiss a banded appearance at the outcrop scale. The elongate minerals, including micas, define an ENE-trending lineation ($075^{\circ}/12^{\circ}$). Shear bands are locally well developed in the mica-rich horizons, indicating a top-W transport during later stages of the deformation. Parts of the gneiss, however, show no evidence of asymmetric structures and the foliation bends around apparently symmetrical porphyroblasts of plagioclase. Several map-scale ductile shear zones cut the mylonitic gneiss forming asymmetric lenses at the scale of 3–10 m. Most of these shear zones show top-W kinematics, although some show top-E movement indicating a component of shortening across the foliation.

Quartz veins and minor shear zones

Quartz veins, 1–40 cm thick and continuous up to 15 m along strike, cut through both the L>S eclogite with the associated kyanite and amphibole veins, and the foliated eclogites (Fig. 2b,c). The quartz veins are consistently N–S-trending (Fig. 5f) and have an amphibolitized zone of up to 0.5 m into the wall rock. The highest concentration of quartz veins is observed in the main L>S eclogite tectonite (Fig. 2b), while the mylonitic gneiss only has minor 1–3 cm thick, up to 1 m long, quartz veins. The quartz veins are composed of mega-crystic, quartz crystal aggregates, and opened during dominantly E–W extension.

A set of shear zones cutting the eclogite facies lineation and the eclogite to amphibolite facies foliation at a high angle (Figs 2b,c & 3e) also locally affects the quartz veins (Fig. 3f). The shear zones are defined by deflection of the foliation and lineation in a 5–20 cm wide zone adjacent to the shear zones that often have a brittle fracture along its trace. The shear zones are up to 1.5 m in length and cause retrogression of the eclogite. They constitute a conjugate set with both dextral and sinistral movement (Fig. 5g), with average orientation $210^{\circ}/70^{\circ}$ and $345^{\circ}/80^{\circ}$ respectively. The orientation and relative movement are consistent with shortening along the bisectrix of the acute angle between the conjugate shears.

MINERAL CHEMISTRY

Mineral analyses were performed on a Cameca Camebax electron microprobe at the Mineralogical–Geological Museum, University of Oslo. Data reduction was done with the Cameca PAP software package. The accelerating voltage was 15 kV and the counting time was 10 s (increased for minor elements). Point analyses of garnet and pyroxene (20 nA) were performed. Amphibole, mica, epidote and feldspar were analysed

with a defocused beam (10 nA). Synthetic and natural minerals and oxides were used as standards.

Garnet from the three different structural types of eclogites and the amphibolites is rich in almandine (Alm_{44-57}), with grossular₁₇₋₃₀, pyrope₁₄₋₃₅ and spessartine_{0.7-3.2}. Garnet of the different fabrics eclogite shows zonation of high CaO, high X_{FeO} ($\text{FeO}/(\text{FeO} + \text{MgO})$, oxides in wt%) and low MgO cores; this is most distinct in the L>S-tectonite (Fig. 6a,b) which also shows high FeO in the cores (Table 2). Concentric zoning of the L>S eclogite garnet locally shows a bell-shaped MnO profile (Fig. 6a). The high MnO occurs in the core of the garnet, but also as an inclusion of older MnO-rich garnet (Fig. 6b). Chemical zoning with similar chemistry as the rim also follows fractures and linear structures, often without visible fractures into the garnet (Fig. 6c), similar to those recorded from the Bergen Arcs by Erambert & Austrheim (1993).

Garnet in the amphibolites is similar to that in the eclogites, except for an increase of Fe and Mn in parts of the rims. The amphibolite garnet shows complex zoning with chemical relicts of the eclogite facies garnet (Fig. 6d). The cores have small areas with high FeO, MnO, CaO, low MgO and high X_{FeO} ratio of up to 0.83 (Table 2), while most of the core shows lower FeO, higher MgO and CaO contents. The anhedral grain boundaries and the complex zonation indicate resorption of the older garnet, whereas the increase in FeO, MnO and decrease in MgO locally along the rim show equilibrium in amphibolite facies.

Pyroxene from the different eclogites described above is classified as omphacite (Table 3; classification after Morimoto, 1988; Fe^{3+} calculated after Neumann, 1976). Omphacite of the L>S eclogite is Jd_{48-49} , with a Na_2O content of *c.* 7 wt%, and low aegerine content. The omphacite of the foliated eclogite shows Jd_{46-50} , Ae_{10} and Na_2O content of up to 9 wt%. The omphacite of the mylonitic eclogite has a Na_2O content of 6.5–7.0 wt%. Aegerine varies up to $\text{Ae}_{5.5}$ and corresponds to a variation Jd_{39-48} .

Amphibole is calcic and sodic–calcic (Table 4, classification after Leake, 1997). The most abundant eclogite facies amphibole in the L>S eclogite is barroisite, while actinolite also occurs in this eclogite. The amphibole veins of the L>S eclogite also contain barroisite. Amphibole inclusions in garnet of the L>S eclogite are barroisite, while the green amphibole not connected to zonation fractures shows considerably higher X_{FeO} . The foliated eclogites have only minor amounts of magnesiotaramite, while mylonitic eclogite includes barroisite, both as smaller grains and large porphyroblasts. Green amphibole in the retrograde amphibolites ranges in composition from magnesiohornblende through tschermakite to ferropargasite.

Sheet silicates White mica, commonly phengite, is present in all the rock types at Vårdalsneset. The Si content of the phengite varies between 6.52 and 6.74 a.f.u., highest in the felsite (Table 5). The (Mg + Fe)

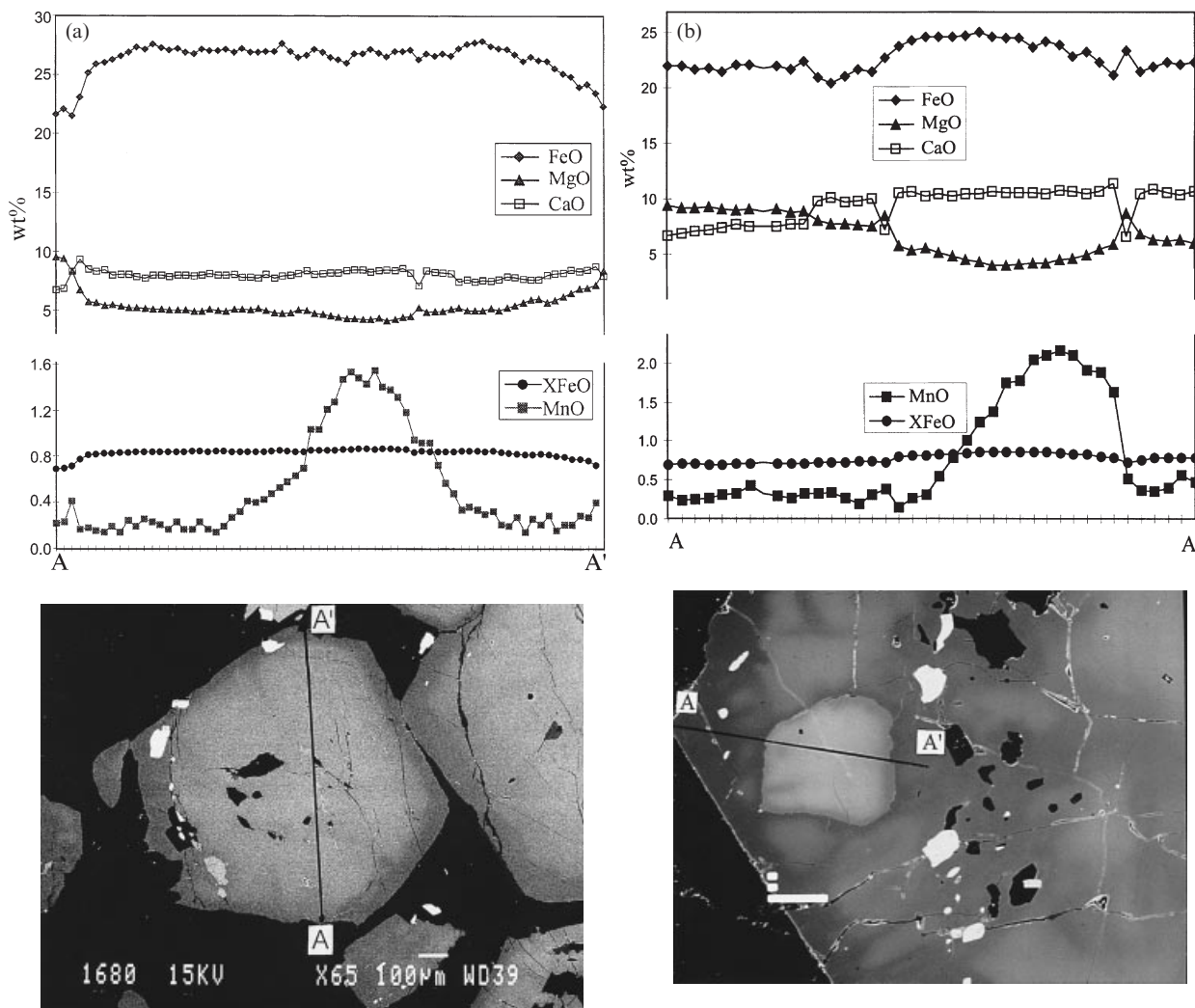


Fig. 6. BSE photomicrographs and zoning profiles of garnet. (a) Zoning profile across an euhedral garnet of the L>S eclogite. The profile is concentric and shows a bell-shaped MnO profile in the core region and increasing MgO, decreasing FeO, CaO and X_{FeO} in the rim. Profile 9, sample V5B, scale bar is 100 μm . (b) Zoning profile across MnO-rich garnet fragment in the euhedral garnet of the L>S eclogite. The profile shows a bell-shaped MnO-profile of the garnet fragment, a decrease of FeO, CaO and X_{FeO} and increase of MgO outside the fragment. Profile 3, sample V5B, scale bar is 100 μm .

content of the phengite is 0.70–0.88 for the eclogites and felsites, and about 0.66 in the mylonitic gneiss. In addition to the phengite, the L>S eclogite also contains paragonite and small amounts of talc. Margarite occurring in the retrogressed part of the kyanite-rich L>S-eclogite has $\text{Na}=0.39$ a.f.u. Biotite is present in the amphibolite and the granodioritic gneiss. The biotite in the amphibolites has X_{Fe} ($\text{Fe}/(\text{Fe} + \text{Mg})$ ratio, a.f.u.) of 0.40. The biotites in the mylonitic gneiss is higher in iron, and has $X_{\text{Fe}}=0.69$.

METAMORPHIC EVOLUTION

Pre-eclogite facies

Protoliths to the eclogites at Vårdalsneset are not present, but high CaO content in garnet cores may

indicate breakdown of plagioclase. Inclusions of plagioclase, green amphibole, epidote and quartz occurring in the cores of garnet may be remnants of an amphibolite facies mineralogy. Garnet zonation showing a locally bell-shaped MnO profile and prograde X_{FeO} indicate also that the Vårdalsneset eclogite evolved by prograde metamorphism. This was previously suggested from several eclogites in Sunnfjord by Krogh (1980, 1982) and Cuthbert & Carswell (1990). Thermometry on amphibole inclusions in garnet gives $T=490 \pm 63$ °C (Graham & Powell, 1984; $\text{Fe}_{\text{amphibole}} = \text{Fe}^{2+}$) for the pre-eclogite facies stage.

Eclogite facies

Pressure and temperature for the formation of eclogite at Vårdalsneset are estimated based on the phengite

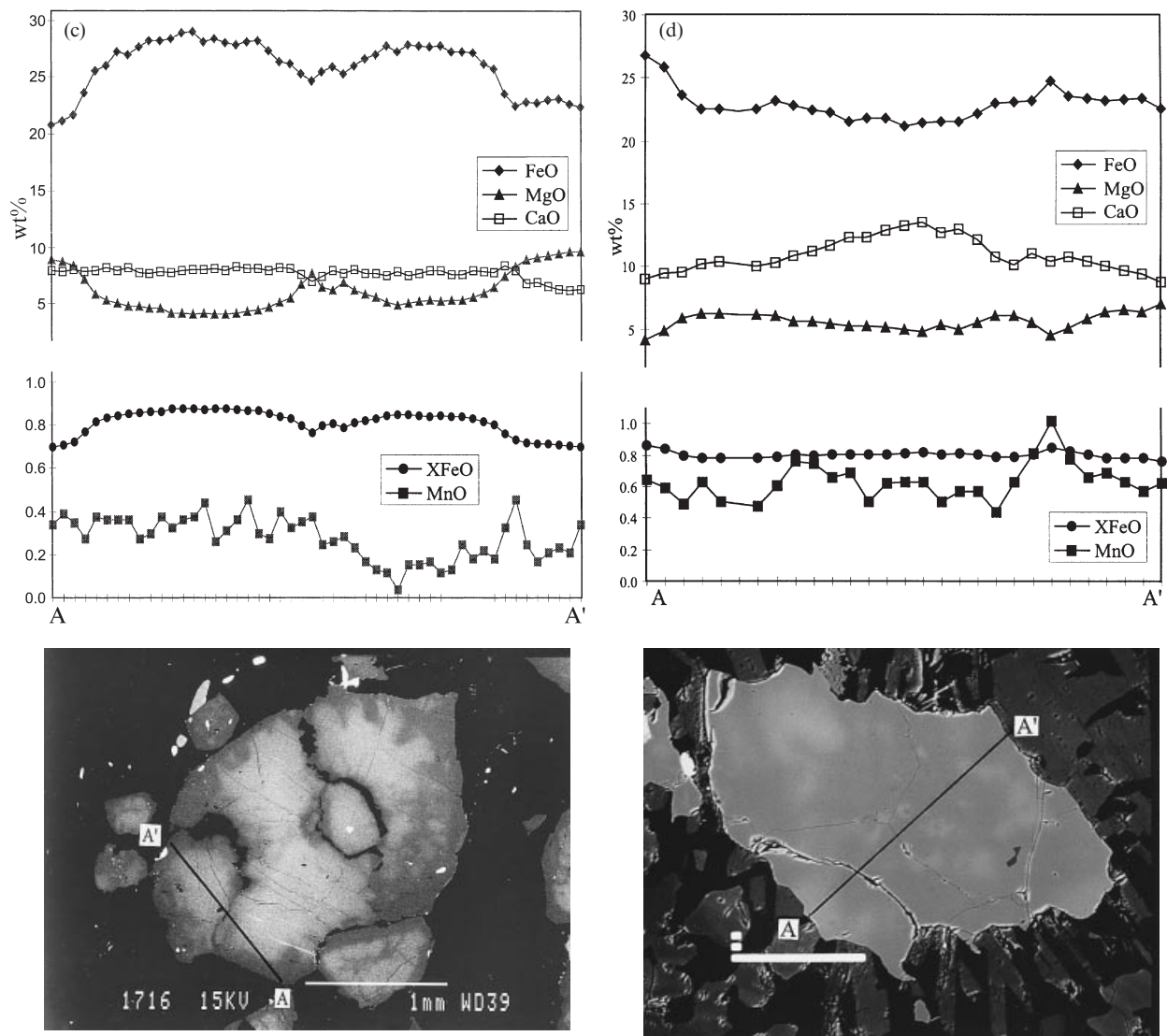


Fig. 6. *Cont'd.* (c) Zoning profile across a zonation vein following a fracture in the garnet of L>S eclogite. Zonation along rim and of the vein shows decrease in FeO, CaO and X_{FeO} and increase of MgO. Profile 7, sample V5B. (d) Zoning profile through anhedral garnet of the amphibolite illustrating complex zoning of the core and local high FeO and X_{FeO} in the rim. Profile 5, sample V34, scale bar is 100 μm .

geobarometer after Waters & Martin (1993) and the Grt–Cpx geothermometer after Powell (1985). P – T estimates were carried out for the L>S-tectonite and mylonitic eclogite of equilibrated rim compositions in contact. Analyses of phengite, garnet and clinopyroxene of the L>S-tectonite eclogite and the mylonitic eclogite gave $T = 677 \pm 21$ °C, $P = 16 \pm 2$ kbar and $T = 691 \pm 20$ °C, $P = 15 \pm 1.5$ kbar, respectively, identical within the uncertainties. This is a higher temperature estimate than those earlier proposed from the Sunnfjord region (Fig. 1; Krogh, 1980; Griffin *et al.*, 1985). However, the estimates show lower pressure and temperature compared to those from the Nordfjord area (Fig. 1) using the same geothermobarometers Wain (1997), still supporting the temperature distribution outlined by Griffin *et al.* (1985) through WGR.

Amphibolite facies

Symplectitic plagioclase and amphibole are characteristic of the amphibolites, demonstrating that they formed from eclogites during decompression and hydration (Bryhni, 1966; Krogh, 1980). Krogh (1980) also described breakdown of rutile to ilmenite and phengite to biotite as a transition from the eclogite to amphibolite facies assemblages, similar to observations from Vårdalsneset.

Both the garnet and amphibole of the amphibolites show a complex chemical variation and zonation. After detailed studies of mineral zoning, temperature estimates based on the garnet–amphibole geothermometer after Graham & Powell (1984) were attempted on amphibolite with well-equilibrated, subhedral amphi-

Table 2. Representative mineral chemical analyses of garnet.

Rock type	L > S eclogite				Foliated eclogite		Mylonitic eclogite		Amphibolite		
	V5B	V5B	V5B	V5B	V17	V17	V41	V41	V46	V46	V46
Sample	1.1	9–40	1	2	1.3c	1	3.1	12	10	1.2	1.1
Analyses	core	core	rim	rim	core	rim	core	rim	core light	core dark	rim light
SiO ₂	38.91	37.75	39.67	39.98	38.77	39.19	39.68	40.28	38.45	38.87	38.21
TiO ₂	0.08	0.15	0.01	0.01	0.10	0.02	0.05	0.03	0.01	0.14	0.08
Al ₂ O ₃	21.07	20.72	21.70	21.84	21.05	21.39	21.71	21.87	21.29	21.35	20.98
FeO	23.97	26.83	22.08	22.62	25.55	25.04	21.01	21.25	24.21	21.69	24.62
MnO	0.41	1.55	0.37	0.35	0.52	0.49	0.42	0.51	0.95	0.69	0.98
MgO	4.66	4.33	7.94	9.26	3.72	6.61	7.45	8.97	5.85	7.29	5.00
CaO	10.80	8.37	8.62	6.48	10.90	7.61	9.97	7.87	8.43	9.34	9.42
Total	99.90	99.70	100.39	100.53	100.61	100.34	100.29	100.78	99.19	99.37	99.29
Structural formula based on 8 cations											
Si	3.03	2.98	3.02	3.03	3.02	3.02	3.02	3.04	3.01	3.00	3.00
Ti	0.00	0.01	0.00	0.00	0.01	0.00	0.00	0.00	0.00	0.01	0.01
Al	1.93	1.93	1.95	1.95	1.93	1.94	1.95	1.94	1.96	1.94	1.94
Fe ²⁺	1.56	1.77	1.40	1.43	1.66	1.61	1.34	1.34	1.58	1.40	1.62
Mn	0.03	0.10	0.02	0.02	0.03	0.03	0.03	0.03	0.06	0.05	0.07
Mg	0.54	0.51	0.90	1.05	0.43	0.76	0.85	1.01	0.68	0.84	0.59
Ca	0.90	0.71	0.70	0.53	0.91	0.63	0.81	0.64	0.71	0.77	0.79
Alm	51.5	57.3	46.3	47.3	54.7	53.2	44.2	44.4	52.2	45.8	52.8
Grs	29.7	23.0	23.2	17.4	29.9	20.7	26.9	21.1	23.3	25.3	25.9
Prp	17.9	16.5	29.7	34.6	14.2	25.0	28.0	33.4	22.5	27.4	19.1
Sps	0.9	3.2	0.8	0.7	1.1	1.1	0.9	1.1	2.1	1.5	2.1
X _{FeO}	0.84	0.86	0.74	0.71	0.87	0.79	0.74	0.70	0.81	0.75	0.83

Abbreviations after Kretz (1983).

bole crystals. The amphiboles show an abrupt rim zonation along grain boundaries with increasing FeO and decreasing MgO, the change in chemistry being correlated to introduction of fluids by the numerous quartz veins cutting the eclogite. The complex garnet zoning of the amphibolites is described above, and the high FeO rim of the garnet is assumed to be in equilibrium with the amphibole cores. Calculations give $T = 564 \pm 44$ °C ($Fe_{\text{amphibole}} = Fe^{2+}$), indicating a decreasing temperature during decompression. The same temperature calculations using the amphibole rim composition gives *c.* 920 °C, which is regarded as unrealistic, and explained by the fluid interaction along grain boundaries and fractures of amphiboles not affecting the less diffusive garnet.

Margarite is produced by breakdown of kyanite in the L > S-eclogite during amphibolitization. Margarite production in anorthosite described further north in the WGR took place at < 610 °C and 8.2 kbar (Cotkin *et al.*, 1988). The reaction $Zo + Ky + V \rightarrow Mg + Qtz$ takes place along the univariant line between 10.3 and 8.1 kbar and 450–610 °C according to Perkins *et al.* (1980). Fractures through kyanite are channelling fluids and are filled by the margarite. In microscale they can be traced outside the kyanite and show orientations similar to the quartz veins. The *P–T* estimates indicated above give maximum conditions for the introduction of the quartz.

The mylonitic gneiss exposed at Vårdalsneset is dominated by plagioclase-bearing assemblages showing an amphibolite facies mineralogy. The high Si content of 6.52–6.67 indicates a minimum pressure of the

Table 3. Representative mineral chemical analyses of pyroxene.

Rock type	L > S eclogite		Foliated eclogite		Mylonitic eclogite	
	V5B	V17	V17	V41	S6	
Sample	1.2	1.1	2	2.3	4	
Analyses						
SiO ₂	57.27	57.23	56.88	57.21	56.71	
TiO ₂	0.03	0.06	0.08	0.03	0.07	
Al ₂ O ₃	11.59	12.73	11.55	10.85	9.62	
FeO	2.78	3.96	4.31	2.98	3.14	
MnO	0.01	0	0.03	0	0.01	
MgO	8.54	6.88	7.56	8.6	9.52	
CaO	13.29	11.21	12.16	13.47	14.96	
Na ₂ O	7.25	8.91	8.25	6.97	6.56	
Cr ₂ O ₃	0.04	0.07	0.07	0.02	0.04	
Total	100.8	101.05	100.89	100.13	100.63	
Structural formula based on 4 cations						
Si	2.00	1.99	1.99	2.02	1.99	
Ti	0.00	0.00	0.00	0.00	0.00	
Al(tot)	0.48			0.45		
Al ^{IV}		0.01	0.01		0.01	
Al ^{VI}		0.51	0.46		0.39	
Cr	0.00	0.00	0.00	0.00	0.00	
Fe ³⁺	0.00	0.10	0.10	0.00	0.05	
Fe ²⁺	0.08	0.02	0.02	0.09	0.04	
Mn	0.00	0.00	0.00	0.00	0.00	
Mg	0.45	0.36	0.39	0.45	0.50	
Ca	0.50	0.42	0.45	0.51	0.56	
Na	0.49	0.60	0.56	0.48	0.45	
Morimoto (1988)						
Jd	48.6	50.3	45.7	47.6	39.3	
Ae	0.5	10.0	10.4	0.00	5.5	
Q	51.0	39.8	43.9	52.4	55.2	
	Omp	Omp	Omp	Omp	Omp	

Abbreviations after Kretz (1983).

phengite formation in the gneiss of 7–10 kbar assuming a temperature of 400–700 °C (Massonne & Schreyer, 1987). The phengite may be a relict of the earlier higher pressure metamorphism of the gneiss.

Table 4. Representative mineral chemical analyses of amphibole.

Rock type	L > S eclogite					Amphibole vein	Foliated	Mylonitic	Amphibolite			
	V5B	V5B	V5B	V5B	V5B	L > S eclogite	eclogite	eclogite	V34	V34	V46	V46
Sample	V5B	V5B	V5B	V5B	V5B	V12	V17	S6	V34	V34	V46	V46
Analyses	6.2	3.1a	1.15a	11.4	7.5	3.5a	2.2	1.2	5.3	1a.2	1.4	6.4
				inclusion in Grt	inclusion in Grt, along fracture with zonation				rim	core		
SiO ₂	52.75	54.74	57.73	47.48	52.63	54.46	43.27	54.31	47.52	41.59	38.17	45.45
TiO ₂	0.14	0.08	0.03	0.29	0.14	0.13	0.19	0.11	0.17	0.08	0.09	0.5
Al ₂ O ₃	9.37	9.45	0.55	13.05	9.4	9.17	16.23	9.1	9.74	15.72	19.26	14.36
FeO (total)	6.57	4.76	6.09	11.96	6.56	5.52	11	5.5	13.09	17.2	18.77	12.78
MnO	0.02	0.09	0.14	0	0.05	0.01	0.05	0	0.27	0.32	0.37	0.16
MgO	16.6	16.86	19.66	11.97	16.76	16.39	12.19	16.48	13.46	8.23	6.16	11.43
CaO	7.98	7.4	13.32	7.93	8.32	7.53	9.64	8.44	11.16	11.8	11.5	9.31
Na ₂ O	3.58	4.02	0.13	4.08	3.03	3.96	3.63	3.09	1.39	1.6	1.9	2.61
K ₂ O	0.2	0.1	0.01	0.32	0.12	0.1	1.08	0.16	0.33	0.6	0.66	0.5
Cl	0.01	–	–	0	–	–	0.01	0	0.02	0.04	0.15	0.14
Σ	97.22	97.5	97.66	97.08	97.01	97.27	97.29	97.19	97.15	97.18	97.03	97.24
O = Cl	–	–	–	–	–	–	–	–	–	–	0.03	0.03
Total	97.22	97.5	97.66	97.08	97.01	97.27	97.29	97.19	97.15	97.18	97.00	97.21
Structural formula based on sum-(Na + K + Ca) = 13, analysis V5B-1.15a based on 23 O												
Si	7.28	7.48	8.03	6.79	7.25	7.50	6.25	7.48	6.84	6.21	5.76	6.52
Ti	0.01	0.01	0.00	0.03	0.01	0.01	0.02	0.01	0.02	0.01	0.01	0.05
Al ^{IV}	0.72	0.52	0.09	1.21	0.75	0.50	1.75	0.52	1.16	1.79	2.24	1.48
			total									
Al ^{VI}	0.80	1.00		0.99	0.77	0.99	1.02	0.96	0.49	0.97	1.19	0.95
Fe ³⁺	0.23	0.29		0.54	0.65	0.44	0.84	0.46	0.82	1.70	0.63	0.74
Fe ²⁺	0.53	0.25	0.71	0.89	0.10	0.19	0.49	0.18	0.75	0.44	1.74	0.79
			total									
Mn	0.00	0.01	0.02	0.00	0.01	0.00	0.01	0.00	0.03	0.04	0.05	0.02
Mg	3.41	3.43	4.08	2.55	3.44	3.36	2.63	3.39	2.89	1.83	1.39	2.45
Ca	1.18	1.08	1.98	1.22	1.23	1.11	1.49	1.25	1.72	1.89	1.86	1.43
Na	0.96	1.01	0.04	1.13	0.81	1.06	1.02	0.83	0.39	0.46	0.56	0.73
K	0.04	0.02	0.00	0.06	0.02	0.02	0.20	0.03	0.06	0.11	0.13	0.09
Total	15.16	15.17	14.94	15.40	15.06	15.19	15.71	15.09	15.17	15.46	15.54	15.25
X _{FeO}	0.28	0.22	0.50	0.28	0.25	0.47	0.25	0.49	0.68	0.75	0.53	
Amph	Na–Ca	Na–Ca	Ca	Na–Ca	Na–Ca	Na–Ca	Na–Ca	Na–Ca	Ca	Ca	Ca	Ca
	barroisite	barroisite	Act	barroisite	barroisite	barroisite	Mg-taramite	barroisite	Mg-Hbl	Ts	Fe-Prg	Mg-Hbl

Abbreviations after Kretz (1983), in addition Amph, amphibole.

DISCUSSION

Eclogite facies coaxial deformation

The detailed structural mapping of the Vårdalsneset eclogite is regarded as an important small-scale documentation of relations observed over larger parts of the WGR. Large parts of the Vårdalsneset eclogite comprise a tectonite with a sub-horizontal pervasive lineation trending about 030°, consistent with measurements of lineation of other eclogite lenses in the Dalsfjord area. The opening and deformation of eclogite facies extensional veins with constant stretching direction are related to continuous deformation in the same strain regime; no asymmetrical textures or structures associated with formation of the L > S-tectonite have been identified. We therefore argue, in agreement with Andersen *et al.* (1994), that the L > S-tectonite was formed during a stage of coaxial deformation at eclogite facies conditions. Preservation of eclogite facies lineation in eclogite lenses is common in the WGR. As shown for the Vårdalsneset eclogite as well as a larger part of the WGR, the early eclogite lineation is preserved at a high angle to secondary

eclogite or amphibolite facies foliations and stretching lineations in the surrounding rocks (Andersen & Jamtveit, 1990; Dransfield, 1994). All decompression-related fabrics are later rotated due to large-scale folding of the area (Skjerlie, 1969; Torsvik *et al.*, 1986; Krabbendam & Dewey, 1998). Based on the preserved high angle between the early eclogite facies L > S-tectonite, the later eclogite to amphibolite facies flattening fabric and the detachment-related structures which most likely formed in a sub-horizontal orientation (see below), we suggest that the L > S-tectonite is related to crustal thickening during the Caledonian collision (Andersen *et al.*, 1991, 1994).

The eclogite protolith at Vårdalsneset is not preserved. Estimates of 490 ± 63 °C based on inclusions in garnet are taken to represent the pre-eclogite stage (Fig. 7, stage 1), while the L > S eclogite tectonite equilibrated at 677 ± 21 °C and 16 ± 2 kbar (Fig. 7, stage 2). The chemical zoning of garnet from the L > S-tectonite is thought to reflect a two-stage evolution during early subduction and eclogitization. (1) The core with high X_{FeO} and locally bell-shaped MnO concentration reflects a growth zonation caused by fractionation of Mn into the garnet core during

Table 5. Representative mineral chemical analyses of shhet silicates.

Rock type	L>S eclogite				Foliated eclogite	Mylonitic eclogite	Felsite	Amphibolite		Granodioritic gneiss		
	V5B	V5B	V5B	V5B	V17	S6	V34	V34	V21	V50	V50	V50
Sample Analyses	1.12a	1.4	1.5	2	3.1	1.1	5	5.4	1.1a	1.1	1.3	1.2
SiO ₂	63.05	47.08	49.20	50.15	50.27	50.99	50.25	36.78	31.02	48.53	47.45	35.65
TiO ₂	0.01	0.07	0.40	0.26	0.37	0.19	0.30	1.40	0.00	0.74	0.69	2.76
Al ₂ O ₃	0.53	39.94	30.27	28.68	28.46	27.95	28.12	16.59	49.82	25.61	27.31	15.79
FeO	3.06	0.36	1.17	1.18	1.22	1.24	1.70	16.19	0.35	7.08	6.60	24.94
MnO	0.03	0.04	0.00	0.02	0.19	0.07	0.01	0.18	0.00	0.15	0.13	0.66
MgO	28.76	0.18	2.89	3.36	3.40	3.60	3.21	13.42	0.59	2.09	1.79	6.29
CaO	0.03	0.35	0.04	0.01	0.02	0.02	0.00	0.05	11.84	0.00	0.00	0.00
Na ₂ O	0.07	7.03	0.76	0.94	0.78	0.63	0.77	0.20	1.53	0.16	0.22	0.10
K ₂ O	0.01	0.97	10.49	10.23	10.25	10.64	9.73	9.30	0.01	11.24	11.23	9.89
Cr ₂ O ₃	0.00	0.00	0.03	0.05	0.67	0.12	0.05	0.00	–	0.00	0.04	0.00
BaO	–	0.03	0.50	0.44	0.56	0.45	0.41	0.13	–	0.17	0.26	0.09
Total	95.55	96.05	95.75	95.32	96.19	95.90	94.55	94.24	95.16	95.77	95.72	96.17
Structural formula based on 22 O												
Si	8.04	5.98	6.54	6.68	6.66	6.76	6.74	5.58	4.12	6.67	6.52	5.58
Ti	0.00	0.01	0.04	0.03	0.04	0.02	0.03	0.16	0.00	0.08	0.07	0.32
Al	0.08	5.98	4.74	4.50	4.45	4.37	4.44	2.97	7.81	4.15	4.42	2.91
Cr	0.00	0.00	0.00	0.01	0.07	0.01	0.01	0.00	0.00	0.00	0.00	0.00
Fe (total)	0.33	0.04	0.13	0.13	0.14	0.14	0.19	2.06	0.04	0.81	0.76	3.26
Mn	0.00	0.00	0.00	0.00	0.02	0.01	0.00	0.02	0.00	0.02	0.02	0.09
Mg	5.47	0.03	0.57	0.67	0.67	0.71	0.64	3.04	0.12	0.43	0.37	1.47
Ca	0.00	0.05	0.01	0.00	0.00	0.00	0.00	0.01	1.69	0.00	0.00	0.00
Na	0.02	1.73	0.20	0.24	0.20	0.16	0.20	0.06	0.39	0.04	0.06	0.03
K	0.00	0.16	1.78	1.74	1.73	1.80	1.66	1.80	0.00	1.97	1.97	1.97
Ba	–	0.00	0.03	0.02	0.03	0.02	0.02	0.01	0.00	0.01	0.01	0.01
Total	13.93	13.97	14.03	14.0	14.01	14.01	13.94	15.70	14.17	14.18	14.21	15.64
X _{Fe}	0.06	0.53	0.19	0.16	0.17	0.16	0.23	0.40	0.25	0.66	0.67	0.69
Fe + Mg	5.79	0.07	0.70	0.80	0.81	0.85	0.83	5.09	0.16	1.24	1.13	4.73
Mineral	Tlc	Pg	Phg	Phg	Phg	Phg	Phg	Bt	Mrg	Phg	Phg	Bt

Abbreviations after Kretz (1983), in addition Phg, phengite.

prograde growth. Together with the inclusions, the MnO zonation indicates preservation of the core from amphibolite facies. Inclusion of the MnO-rich garnet (Fig. 6b) is thought to represent a fragment of garnet grown in the early amphibolite facies stage. The fragmented appearance may indicate that garnet porphyroblasts were broken up during early stages of crustal thickening, later overgrown and preserved during eclogitization. (II) The abrupt change in garnet composition along rim, fractures and linear structures reflects the metamorphic transition to the eclogite facies assemblage during introduction of a fluid phase associated with the eclogitization. Garnet rims as well as margins of micro fractures in garnet are low in X_{FeO} and include the eclogite assemblage. These observations are interpreted as prograde growth zonation at eclogite facies conditions. The change in chemistry along fractures extending into the cores of some garnet reflects a diffusion process during the fluid introduction. A high fluid pressure during formation of the L>S eclogite seems likely because of the high content of the hydrous phases and the common occurrence of eclogite facies veins. A high fluid pressure may also enhance fracturing of the garnet. The oblong orientation of garnet parallel to the lineation of the L>S-tectonite and modification of garnet cores along fractures perpendicular to the same lineation link the formation of the zoning fractures to the deformation during formation the L>S-tectonite.

Eclogite and amphibolite facies flattening and shear zones

As shown above, the Vårdalsneset eclogite experienced a secondary eclogite facies deformation event, characterized by E–W-striking foliation, conjugate eclogite facies shear zones and micro shear bands showing both top-E and top-W movement. These structures truncate the original NNE–SSW-trending lineation (Fig. 7, stage 3). Conjugate eclogite facies shear zones cutting earlier L>S-tectonites were described by Andersen & Jamtveit (1990) from other eclogites in the Sunnfjord area, indicating a regional distribution of the feature. The symmetry of the lenses, conjugate shear zones and formation of a new foliation indicate that the earlier L>S eclogite was deformed in a dominantly non-rotational strain-regime accompanied by E–W stretching. The common preservation of the orientation of the earlier L>S fabric in different eclogite lenses with variable aspect ratios also indicates coaxial deformation at the second eclogite facies event. The high angle between the fabrics during the two eclogite facies events indicates a drastic change in the deformation regime from initial compression during crustal thickening to E–W-stretching during crustal thinning.

An exception to the coaxial fabrics described and interpreted above is represented by the E–W-trending mylonite zone, which is developed both in granodioritic gneisses and eclogite. We suggest that the mylonite

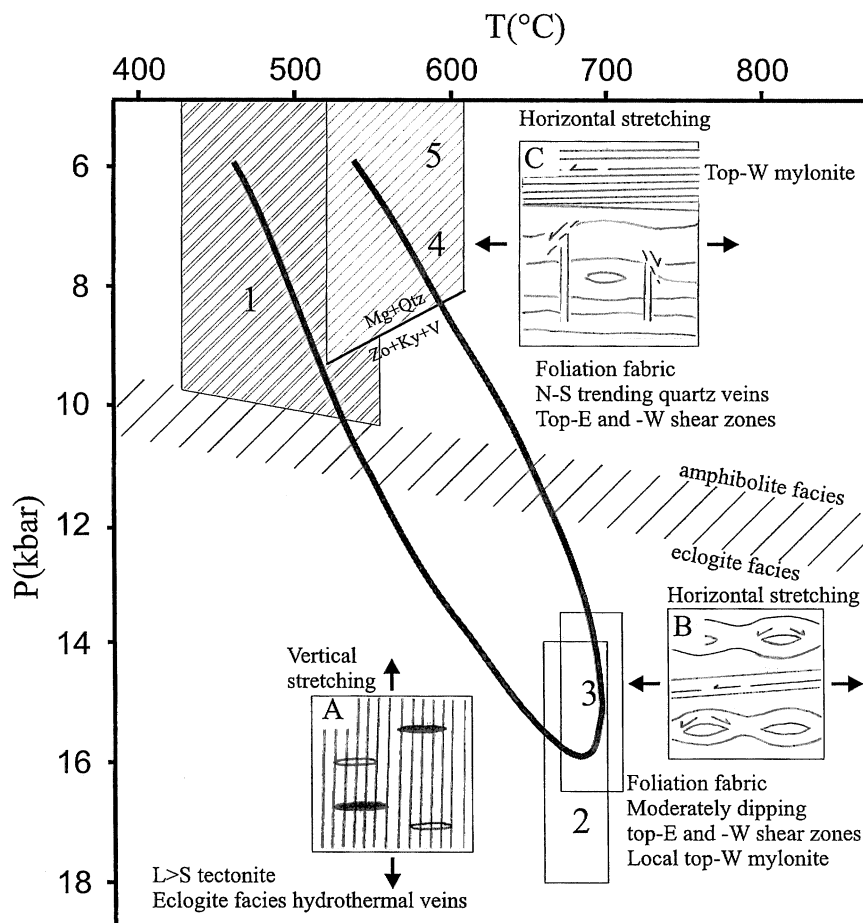


Fig. 7. Pressure, temperature and structural evolution for the Vårdalsneset eclogite. Boxes numbered 1–5 indicate P – T conditions for the five tectono-metamorphic stages described in the text. Boxes A, B and C indicate the bulk strain regime and characteristic structures developed.

zone was formed during non-coaxial deformation with dominantly top-W movement as indicated by the kinematic indicators described above. Andersen *et al.* (1994) assumed that all the mylonites at Vårdalsneset were formed at amphibolite facies conditions. In this work, we demonstrate that a part of the mylonite has preserved a syn-kinematic eclogite developed at $T = 691 \pm 20^\circ\text{C}$ and $P = 15 \pm 1.5$ kbar. The granodioritic gneiss described above has an amphibolite facies assemblage; however, relic high-Si phengite indicates that the mylonitic deformation of the granodiorite started under higher-pressure conditions in agreement with local preservation of eclogite. The P – T estimates for the L>S and mylonitic eclogite overlap within the uncertainties, showing that both strain regimes occurred deep in the crust. We interpret the change in the strain regime to reflect the transition from burial to exhumation processes.

Amphibolite facies minerals in the amphibolite and felsic horizons are oriented parallel to the eclogite facies foliation, although with variable intensity. An estimate achieved from a foliated and well-equilibrated

amphibolite yields $564 \pm 44^\circ\text{C}$ (Fig. 7, stage 4). As described above, steep N–S-trending quartz veins cut the eclogite and caused amphibolite facies retrogression. The origin of the fluids contributing the large amounts of quartz is not yet known, but according to Heinrich (1982) fluids can be released in felsic gneisses during amphibolitization as phengite reacts to biotite, and cause retrogression of eclogites on entering the mafic lenses. Margarite production along subvertical microfractures through eclogite facies kyanite indicates lowering of the temperature to 450 – 610°C and exhumation to pressures between 10.3 and 8.1 kbar during introduction of the quartz veins. This agrees with the above estimate for the foliated amphibolite. The orientation of the quartz veins, the occurrences of amphibolite facies conjugate shear zones and the conformity between amphibolite and the second-stage eclogite foliations indicate no major change in orientation of the principal strain axes from E–W-stretching and vertical shortening at eclogite facies to the deformation at amphibolite facies condition. Thus, we suggest that the initial decompression from eclogite to

amphibolite facies conditions took place in a dominantly coaxial strain regime where the lower crust underwent vertical shortening and horizontal E–W-stretching.

Andersen *et al.* (1994) related the secondary coaxial strain regime (stages 3–4 described above) to the exhumation of deep crustal rocks during the late-orogenic extension of the Caledonides. However, they related the coaxial E–W-stretching fabrics solely to the amphibolite facies, while we have demonstrated here that the shift in strain regime occurred at eclogite facies, earlier than previously recognized. Other studies in the Sunnfjord area (Andersen & Jamtveit, 1990; Engvik, 1996) shows that the coaxial E–W-stretching and vertical shortening during amphibolitization was regionally important in the area, implying that this strain regime characterized a significant part of the *P–T* space through which the Sunnfjord eclogites were exhumed.

The mylonites cutting the Vårdalsneset eclogite and surrounding rocks are related to the Nordfjord-Sogn Detachment (NSD; Fig. 1) (Andersen *et al.*, 1994). The NSD represents the principal extensional shear zone in the SW Norwegian Caledonides (Norton, 1987; Andersen, 1998). According to the previous studies (Swensson & Andersen, 1991), the mylonites of the detachment in the Dalsfjord area show a consistent top-W movement and were developed continuously from amphibolite to greenschist facies conditions (Fig. 7, stage 5). The local occurrence of eclogite facies mylonites at Vårdalsneset situated in the lowermost part of the detachment zone may indicate that non-coaxial deformation commenced at higher pressure conditions. Eclogite facies mylonites are also present on the south side of Dalsfjorden (Engvik, 1996), but these mylonites show no consistent sense of shear.

Geodynamic implications

The pervasive coaxial deformation during uplift of WGR indicates a more complex exhumation model than the simple shear model proposed by Norton (1987). Although more complex, the structural and metamorphic evolution of the Vårdalsneset eclogite described in this study supports the exhumation models involving lower crustal coaxial thinning and middle to upper crustal detachment faulting (Andersen & Jamtveit, 1990; Dewey *et al.*, 1993; Jolivet *et al.*, 1994). Thrust imbrication is proposed as an explanation for juxtaposition of eclogites formed at different pressure conditions in the Nordfjord area (Wain, 1997). This process cannot be excluded as taking part in the exhumation mechanism from UHP to HP conditions, but so far no contractional high-strain zone related to deep crustal thrust imbrication internally in WGR has been reported. However, metastable preservation of Proterozoic gabbros and granulites has been documented from the eclogite areas of WGR both in

Sunnfjord (Engvik, 1996; Engvik *et al.*, in press) and Nordfjord (Austrheim, 1998), showing that rock bodies equilibrated at widely different pressures indeed may occur together.

The driving force for exhumation of the WGR remains speculative. The WGR must, however, have been highly buoyant because of its felsic nature and incomplete reactions under eclogite facies conditions (Engvik *et al.*, 2000). Buoyancy forces acting on subducted large light rock bodies, with minor eclogite lenses, may cause them to rise (England & Holland, 1979; Austrheim, 1991; Platt, 1993). In addition, metamorphism will actively influence geodynamic processes through rheology and density changes (Austrheim, 1998). The Vårdalsneset eclogite is anomalous in this respect, because it was only partly amphibolitized by introduction of fluids as evidenced by retrogression around abundant quartz veins. The more widespread amphibolitization in the WGR in general clearly reduced the density and enhanced its buoyancy.

ACKNOWLEDGEMENTS

We are grateful to H. Austrheim for stimulating discussions and help during this work. We also thank M. Erambert, P. T. Osmundsen and T. Bjerkgård for their help. Careful review and suggestions by H. Stünitz, Neubauer, and one anonymous referee are gratefully acknowledged. Financial support from NFR (Norwegian Research Council) through project 107603/410 'Fluid-induced metamorphism and geodynamic processes', project 440.92/007 'Extension and exhumation of deep crust after the Caledonian orogeneses' and project 128862/410 'Late- to postorogenic evolution of mountain belts' is acknowledged.

REFERENCES

- Andersen, T. B., 1998. Extensional tectonics in the Caledonides of southern Norway, an overview. *Tectonophysics*, **285**, 333–351.
- Andersen, T. B. & Jamtveit, B., 1990. Uplift of deep crust during orogenic extensional collapse: model based on field studies in the Sogn-Sunnfjord region of Western Norway. *Tectonics*, **9**, 1097–1111.
- Andersen, T. B., Jamtveit, B., Dewey, J. F. & Swensson, E., 1991. Subduction and exhumation of continental crust: major mechanisms during continent–continent collision and orogenic extensional collapse, a model based on the south Caledonides. *Terra Nova*, **3**, 303–310.
- Andersen, T. B., Jolivet, L. & Osmundsen, P. T., 1994. Deep crustal fabrics and a model for the extensional collapse of the Southwest Norwegian Caledonides. *Journal of Structural Geology*, **16**, 1191–1203.
- Austrheim, H., 1991. Eclogite formation and dynamics of crustal roots under continental collision zones. *Terra Nova*, **3**, 492–499.
- Austrheim, H., 1998. Influence of fluid and deformation on metamorphism of the deep crust and consequences for the geodynamics of collision zones. In: *When Continents Collide: Geodynamics and Geochemistry of Ultrahigh-Pressure Rocks* (eds Hacker, B. R. & Liou, J. G.), pp. 297–323. Kluwer Academic Publishers, Dordrecht, The Netherlands.

- Avigad, D., 1992. Exhumation of coesite-bearing rocks in the Dora Maira massif (western Alps, Italy). *Geology*, **20**, 947–950.
- Bryhni, I., 1966. Reconnaissance studies of gneisses, ultrabasites, eclogites and anorthosites in Outer Nordfjord, Western Norway. *Norges Geologiske Undersøkelse Bulletin*, **241**, 1–68.
- Chemenda, A., Matte, P. & Sokolov, V., 1997. A model of Paleozoic obduction and exhumation of high-pressure/low-temperature rocks in the southern Urals. *Tectonophysics*, **276**, 217–227.
- Chopin, C., 1984. Coesite and pure pyrope in high grade blueschists of the Western Alps: a first record and some consequences. *Contributions to Mineralogy and Petrology*, **86**, 107–118.
- Cotkin, S. J., Valley, J. W. & Essene, E. J., 1988. Petrology of margarite-bearing meta-anorthosite from Seljeneset, Nordfjord, western Norway: implications for the *P*–*T* history of the Western Gneiss Region during Caledonian uplift. *Lithos*, **21**, 117–128.
- Cuthbert, S. J. & Carswell, D. A., 1991. Formation and exhumation of medium-temperature eclogites in the Scandinavian Caledonides. In: *Eclogite Facies Rocks* (ed. Carswell, D. A.), pp. 180–203. Blackie & Son Ltd, Glasgow.
- Cuthbert, S. J., Harvey, M. A. & Carswell, D. A., 1983. A tectonic model for the metamorphic evolution of the Basal Gneiss Complex, Western South Norway. *Journal of Metamorphic Geology*, **1**, 63–90.
- Dewey, J. F., 1988. Extensional collapse of orogens. *Tectonics*, **7**, 1123–1139.
- Dewey, J. F., Ryan, P. D. & Andersen, T. B., 1993. Orogenic uplift and collapse, crustal thickness, fabrics and metamorphic phase changes: the role of eclogites. *Journal of the Geological Society of London, Special Publication*, **76**, 325–343.
- Dobrzhinetskaya, L. F., Eide, E. A., Larsen, R. B., Sturt, B. A., Trønnes, R., Smith, D. C., Taylor, W. R. & Posukhova, T. V., 1995. Microdiamond in high-grade metamorphic rocks of the Western Gneiss Region, Norway. *Geology*, **7**, 597–600.
- Dransfield, M., 1994. Extensional exhumation of high-grade metamorphic rocks in Western Norway and the Zaskar Himalayas. *PhD Thesis, University of Oxford, Oxford, UK*.
- Engvik, A. K., 1996. Eclogitization and amphibolitization of Holt-Saurdal-Tyssedalsvatnet layered gabbroic complex. *NGU Report 96.133*. Geological Survey of Norway, Trondheim, Norway.
- Engvik, A. K., Austrheim, H. & Andersen, T. B., 2000. Structural, mineralogical and petrophysical effects on deep crustal rocks of fluid-limited polymetamorphism, Western Gneiss Region, Norway. *Journal of the Geological Society of London*, **157**, 121–134.
- England, P. C. & Holland, T. J. B., 1979. Archimedes and the Tauern eclogites: the role of buoyancy in the preservation of exotic eclogite blocks. *Earth and Planetary Science Letters*, **44**, 287–294.
- Erambert, M. & Austrheim, H., 1993. The effect of fluid and deformation on zoning and inclusion patterns in polymetamorphic garnets. *Contributions to Mineralogy and Petrology*, **115**, 204–214.
- Gebauer, D., Lappin, M., Grünenfelder, M. & Wyttenbach, A., 1985. The age and origin of some Norwegian eclogites: a U–Pb zircon and REE study. *Chemical Geology*, **52**, 227–247.
- Griffin, W. L. & Brueckner, H. K., 1980. Caledonian Sm–Nd ages and a crustal origin for Norwegian eclogites. *Nature*, **285**, 319–321.
- Griffin, W. L. & Brueckner, H. K., 1985. REE, Rb–Sr and Sm–Nd studies of Norwegian eclogites. *Chemical Geology*, **52**, 249–271.
- Griffin, W. L., Austrheim, H., Braasted, K., Bryhni, I., Krill, A. G., Krogh, E. J., Mørk, M. B. E., Quale, H. & Tørudbakken, B., 1985. High-pressure metamorphism in the Scandinavian Caledonides. In: *The Caledonide Orogen – Scandinavia and Related Areas* (eds Gee, D. G. & Sturt, B. A.), pp. 783–802. John Wiley & Sons Ltd, Chichester.
- Graham, C. M. & Powell, R., 1984. A garnet–hornblende geothermometer: calibration, testing, and application to the Pelona Schist, Southern California. *Journal of Metamorphic Geology*, **2**, 13–31.
- Heinrich, C. A., 1982. Kyanite-eclogite to amphibolite facies evolution of hydrous mafic and pelitic rocks, Adula Nappe, central Alps. *Contributions to Mineralogy and Petrology*, **81**, 30–38.
- Holland, T. J. B., 1979. High water activities in the generation of high pressure kyanite eclogites of the Tauern Window, Austria. *Journal of Geology*, **87**, 1–27.
- Jolivet, L., Daniel, J. M., Truffert, C. & Goffé, B., 1994. Exhumation of deep-crustal metamorphic rocks and crustal extension in arc and back-arc regions. *Lithos*, **33**, 3–30.
- Kildal, E. S., 1970. *Geologisk kart over Norge, berggrunnskart. Målest.: 1:250 000*. Norges Geologiske Undersøkelse, Trondheim, Norway.
- Krabbendam, M. & Dewey, J. F., 1998. Exhumation of UHP rocks by transtension in the Western Gneiss Region, Scandinavian Caledonides. In: *Continental Transpression and Transtensional Tectonics* (eds Holdsworth, R. E., Strachan, R. A. & Dewey, J. F.), *Geological Society of London Special Publications*, **135**, 159–181.
- Kretz, R., 1983. Symbols for rock-forming minerals. *American Mineralogist*, **68**, 277–279.
- Krogh, E. J., 1980. Geochemistry and petrology of glaucophane-bearing eclogites and associated rocks from Sunnfjord, western Norway. *Lithos*, **13**, 355–380.
- Krogh, E. J., 1982. Metamorphic evolution deduced from mineral inclusions and compositional zoning in garnets from Norwegian country-rock eclogites. *Lithos*, **15**, 305–321.
- Krogh, E. J. & Carswell, D. A., 1995. HP and UHP eclogites and garnet peridotites in the Scandinavian Caledonides. In: *Ultra High Pressure Metamorphism* (eds Coleman, R. G. & Wang, Z.), pp. 244–298. Cambridge University Press, Cambridge, UK.
- Kullerød, L., Tørudbakken, B. O. & Ilebekk, S., 1986. A complication of radiometric age determinations from Western Gneiss Region, South Norway. *Norges Geologiske Undersøkelse Bulletin*, **406**, 17–42.
- Leake, B. E., 1997. Nomenclature of amphiboles: report of the Subcommittee on Amphiboles of the International Mineralogical Association, Commission on New Minerals and Mineral Names. *American Mineralogist*, **82**, 1019–1037.
- Lutro, O., Robinson, P., Solli, A., Tucker, R. B., Wain, A., Terry, M. & Krabbendam, M., 1997. Proterozoic geology of Scandinavian high pressure overprinting in the WGR. *NGU Report 97.132*. Geological survey of Norway, Trondheim, Norway.
- Massonne, H.-J. & Schreyer, W., 1987. Phengite geobarometry based on the limiting assemblage with K-feldspar, phlogopite and quartz. *Contributions to Mineralogy and Petrology*, **96**, 212–224.
- Milnes, A. G., Wenneberg, O. P., Skår, Ø. & Koestler, A. G., 1997. Contraction, extension and timing in the South Norwegian Caledonides: the Sognefjord transect. In: *Orogeny Through Time* (eds Burg, J. P. & Ford, M.), *Geological Society of London Special Publications*, **121**, 123–148.
- Morimoto, N., 1988. Nomenclature of pyroxenes. *American Mineralogist*, **73**, 1123–1133.
- Neumann, E. R., 1976. Two refinement for the calculation of structural formula for pyroxenes and amphiboles. *Norsk Geologisk Tidsskrift*, **56**, 1–6.
- Norton, M. G., 1987. The Nordfjord-Sogn Detachment, W. Norway. *Norsk Geologisk Tidsskrift*, **67**, 93–106.
- Perkins, D., Westrum, E. F. & Essene, E. J., 1980. The thermodynamic properties and phase relations of some minerals in the system CaO–Al₂O₃–SiO₂–H₂O. *Geochimica and Cosmochimica Acta*, **44**, 61–84.
- Platt, J., 1993. Exhumation of high-pressure rocks: a review of concepts and processes. *Terra Nova*, **5**, 119–133.
- Powell, R., 1985. Regression diagnostics and robust regression in geothermometer/geobarometer calibration: the garnet–clinopyroxene geothermometer revisited. *Journal of Metamorphic Geology*, **3**, 231–243.

- Skjerlie, F. J., 1969. The pre-Devonian rocks in the Askvoll-Gaular area and adjacent districts, Western Norway. *Norges Geologiske Undersøkelse Bulletin*, **258**, 325–359.
- Smith, D. C., 1995. Microcoesites and microdiamonds in Norway: an overview. In: *Ultra High Pressure Metamorphism* (eds Coleman, R. G. & Wang, Z.), pp. 299–355. Cambridge University Press, Cambridge, UK.
- Swensson, E. & Andersen, T. B., 1991. Petrography and basement–cover relationships between the Askvoll Group and the Western Gneiss Region, Sunnfjord, W. Norway. *Norsk Geologisk Tidsskrift*, **71**, 15–27.
- Torsvik, T. H., Sturt, B. A., Ramsey, D. M., Kisch, H. J. & Bering, B., 1986. The tectonic implication of Solundian (Upper Devonian) magnetisation of the Devonian rocks of Kvamshesten, western Norway. *Earth and Planetary Science Letters*, **80**, 337–347.
- Torsvik, T. H., Smethurst, M. A., Meert, J. G., van der Voo, R., McKerrow, W. S., Brasier, M. D., Sturt, B. A. & Walderhaug, H. J., 1996. Continental breakup and collision in the Neoproterozoic and Palaeozoic – a tale of Baltica and Laurentia. *Earth Science Review*, **40**, 229–258.
- Tucker, R. D., Råheim, A., Krogh, T. E. & Corfu, F., 1987. Uranium–lead zircon and titanite ages from the northern portion of the Western Gneiss Region, south-central Norway. *Earth and Planetary Science Letters*, **81**, 203–211.
- Wain, A., 1997. New evidence for coesite in eclogite and gneisses: defining an ultrahigh-pressure province in the Western Gneiss region of Norway. *Geology*, **25**, 927–930.
- Waters, D. J. & Martin, H. N., 1993. Geobarometry in phengite-bearing eclogites. *Terra Abstracts*, **5**, 410–411 (updated calibration (1996) at: <http://www.earth.ox.ac.uk/davewa/ecbar.html>).
- Wernicke, B., 1985. Uniform-sense simple shear of the continental lithosphere. *Canadian Journal of Earth Science*, **22**, 108–125.

Received 26 April 1999; revision accepted 12 October 1999.